Kinetics of ^{99m}Tc-Labeled Interleukin-8 in Experimental Inflammation and Infection

Huub J.J.M. Rennen, MSc; Otto C. Boerman, PhD; Wim J.G. Oyen, MD, PhD; and Frans H.M. Corstens, MD

Department of Nuclear Medicine, University Medical Center Nijmegen, Nijmegen, The Netherlands

The cytokine interleukin-8 (IL-8) binds with high affinity to the CXCR1 and CXCR2 receptors on neutrophils. In previous studies, we showed that ^{99m}Tc-IL-8 could rapidly and effectively delineate foci of infection and inflammation in rabbit models of intramuscular infection, colitis, and osteomyelitis. Here, the in vivo kinetics and pharmacodynamics of ^{99m}Tc-IL-8 are studied in detail. A derivative of hydrazinonicotinamide (HYNIC) was used as a bifunctional coupling agent to label the protein with ^{99m}Tc. **Methods:** To address specificity of uptake of ^{99m}Tc-IL-8 in the abscess, uptake in turpentine-induced abscesses in neutropenic rabbits was compared with uptake in turpentine-induced abscesses in normal rabbits. The pharmacokinetics of ^{99m}Tc-IL-8 were studied in neutropenic rabbits and compared with those in normal rabbits. To investigate the interaction of ^{99m}Tc-IL-8 with blood cells in circulation in normal rabbits, the distribution of the radiolabel over circulating white and red blood cells and plasma was determined. The in vivo kinetics of ^{99m}Tc-IL-8 were studied by quantitative analysis of whole-body images acquired between 0 and 6 h after injection. The results of this analysis (in vivo biodistribution) were validated by ex vivo counting of radioactivity in dissected tissues. **Results:** The abscess uptake (percentage of injected dose per gram of tissue [%ID/g] ± SEM) in immunocompetent rabbits (0.41 ± 0.05) was 10 times higher than that in neutropenic rabbits (0.038 ± 0.014), demonstrating specificity of the target uptake of ^{99m}Tc-IL-8. Abscess-to-muscle ratios ± SEM were also 10 times higher (110 ± 10 vs. 10 ± 5). Lung and spleen uptake in normal rabbits was 3 times higher than that in neutropenic rabbits. The blood clearance of the radiolabel in neutropenic rabbits was similar to that in normal rabbits. In circulation, most of ^{99m}Tc-IL-8 (70%) was found in the plasma fraction. Less than one third was associated with red blood cells, and only a very low percentage (<2.5%) was associated with white blood cells. Image analysis revealed a gradually increasing abscess uptake over time up to >15%ID, which was confirmed by ex vivo γ-counting of the infected muscle. The highest increase in uptake in the abscess was observed after 2 h following injection, when most of ^{99m}Tc-IL-8 was cleared from the blood, suggesting specific neutrophil-mediated accumulation of ^{99m}Tc-IL-8 in the abscess. Furthermore, region-of-interest analysis revealed that gradual accumulation of ^{99m}Tc-IL-8 in the abscess was accompanied by a simultaneous clearance of activity from the lungs, suggesting that neutrophil-associated ^{99m}Tc-IL-8 that was initially trapped in the lungs migrates to the abscess at later time points, favoring neutrophil-bound transportation from the lungs to the abscess. **Conclusion:** Substantial support is given for the hypothesis that ^{99m}Tc-IL-8 localizes in the abscess, mainly bound to peripheral neutrophils. Accumulation in the abscess is a highly specific, neutrophil-driven process. As assessed by in vivo and ex vivo analysis, the total fraction that accumulates in the inflamed tissue is extremely high (up to >15 %ID) compared with that of other agents used for imaging infection and inflammation.

Key Words: ^{99m}Tc-labeled interleukin-8; kinetics; inflammation; infection

J Nucl Med 2003; 44:1502–1509

Neutrophils are known to express 2 types of interleukin-8 (IL-8) receptors, CXCR1 and CXCR2, abundantly (*1*). IL-8 binds these receptors with high affinity (0.3–4 nmol/L) (*2*–*5*). The in vivo behavior of radioiodinated IL-8 has been studied in rat (*6*) and rabbit (*7*,*8*) models of infection. In a pilot study, Gross et al. showed that ^{131}I-labeled IL-8 could visualize osteomyelitic lesions in patients (*9*). We have pointed out that the radioiodination method clearly affected the in vivo biodistribution of IL-8 (*10*). For clinical applications, a labeling procedure using the radiometal ^{99m}Tc is preferred over iodine (*10*). Recently, we described the development of a ^{99m}Tc-labeled IL-8 preparation using hydrazinonicotinamide (HYNIC) as a bifunctional coupling agent (*11*). This preparation showed excellent characteristics for imaging infection in 3 different models of infection and inflammation in rabbits (*11*–*13*). In rabbits with intramuscular infection induced by *Escherichia coli*, uptake of ^{99m}Tc-IL-8 in the abscess was rapid and high (*11*). Moreover, ^{99m}Tc-IL-8 showed a remarkably fast clearance from nontarget tissues. Abscess-to-muscle ratios exceeded 100 at 8 h after injection.

In rabbits with chemically induced acute colitis, inflammatory lesions were scintigraphically visualized after injection of either IL-8 or purified granulocytes, both labeled with ^{99m}Tc (*13*). Within a few hours after injection, ^{99m}Tc-IL-8 allowed an adequate evaluation of the inflamed colon. The absolute uptake in the inflamed foci in the colon was much higher for ^{99m}Tc-IL-8 than for ^{99m}Tc-granulocytes.

In a third study, the performance of ^{99m}Tc-IL-8 was evaluated in an experimental model of acute osteomyelitis in rabbits (*12*). The results were compared with those ob-

Received Oct. 25, 2002; revision accepted May 15, 2003.

For correspondence or reprints contact: Huub J.J.M. Rennen, MSc, Department of Nuclear Medicine, University Medical Center Nijmegen, P.O. Box 9101, 6500 HB Nijmegen, The Netherlands.

E-mail: h.rennen@nucmed.umcn.nl

tained using the conventional and well-established agents ^{111}In-granulocytes, ^{67}Ga-citrate, and ^{99m}Tc-methylene diphosphonate (MDP). In this rabbit model of osteomyelitis, ^{99m}Tc-IL-8 clearly delineated the osteomyelitic lesions. Although absolute uptake in the osteomyelitic area was lower than that obtained with ^{67}Ga-citrate and ^{99m}Tc-MDP, the target-to-background ratios were significantly higher for ^{99m}Tc-IL-8.

IL-8 is a proinflammatory chemotactic cytokine. For scintigraphic purposes, protein doses to be administered should be below levels that generate side effects. We showed that a preparation with high specific activity (80 MBq/μg) and high in vitro stability could be prepared when nicotinic acid was used as a coligand (*14*). Imaging doses as low as 70 ng/kg ^{99m}Tc-IL-8 open the way to infection imaging studies in patients.

In this study, 3 fundamental aspects of the in vivo behavior of ^{99m}Tc-IL-8 were investigated: specificity of uptake of ^{99m}Tc-IL-8 in the abscess, mechanism of migration of ^{99m}Tc-IL-8 from the circulation to the inflammatory focus, and kinetics of ^{99m}Tc-IL-8 in vivo.

MATERIALS AND METHODS

Human recombinant IL-8 was kindly provided by Dr. Ivan Lindley (Novartis, Vienna, Austria). Tricine (*N*-[tris(hydroxymethyl)-methyl]glycine) was purchased from Fluka (Buchs); nicotinic acid was from Sigma-Aldrich.

Conjugation of HYNIC to IL-8

The propylaldehyde hydrazone of succinimidyl-hydrazinonicotinamide (HYNIC) was synthesized essentially as described (*15,16*). The IL-8-HYNIC conjugate was prepared as described (*14*). Briefly, in a 1.5-mL vial, 4 μL 1 mol/L $NaHCO_3$, pH 8.2, were added to 35 μL IL-8 (4.8 mg/mL). Subsequently, a 3-fold molar excess of HYNIC in 5 μL dry dimethyl sulfoxide was added dropwise to the mixture. After incubation for 5 min at room temperature, the reaction was stopped by adding an excess of glycine (200 μL, 1 mol/L in phosphate-buffered saline [PBS]). To remove excess unbound HYNIC, the mixture was extensively dialyzed against PBS (0.1- to 0.5-mL dialysis cell, 3,500 molecular weight cutoff; Pierce). Dialyzed samples of approximately 5 μg IL-8-HYNIC were stored at −20°C.

^{99m}Tc Labeling of HYNIC-Conjugated IL-8

Five micrograms IL-8-HYNIC were incubated with 0.2 mL of tricine solution (100 mg/mL in PBS), 25 μL of a freshly prepared tin(II) solution (10 mg $SnSO_4$ in 10 mL nitrogen-purged 0.1N HCl), and 150–350 MBq $^{99m}TcO_4^-$ in saline at room temperature for 30 min. The radiochemical purity was determined by instant thin-layer chromatography (ITLC) on ITLC-SG strips (Gelman Laboratories) with 0.1 mol/L citrate, pH 6.0, as the mobile phase. After the labeling reaction, the reaction mixture was applied to a Sephadex G-25 column (PD-10; Pharmacia) and eluted with 0.5% bovine serum albumin in PBS to purify radiolabeled IL-8. A description of an extensive in vitro characterization (high-performance liquid chromatography, stability, receptor binding assays) has been given elsewhere (*14*).

Animal Studies

All animal experiments were performed in accordance with the guidelines of the local animal welfare committee.

Specificity of Uptake of ^{99m}Tc-IL-8 in Abscess. Neutropenia was induced in 5 female New Zealand White rabbits (2.4–2.7 kg) by intravenous administration of cytarabine (David Bull Laboratories) (50 mg per rabbit per day over 7 d). Routinely, a rabbit model of intramuscular infection induced by *E. coli* is used because it generates a strong leukocytic response and it is a good reflection of a common bacterial infection. In neutropenic rabbits, the immune system is seriously compromised and an infection induced by *E. coli* could have a fatal effect on these animals. For that reason, a sterile turpentine inflammation rather than a bacterial infection was induced. On day 8, a sterile inflammation was induced in the left thigh muscle of these 5 neutropenic rabbits and in a control group of 4 immunocompetent rabbits (0.5 mL of turpentine intramuscularly). During the procedure, rabbits were anesthetized with a subcutaneous injection of a 0.6-mL mixture of 0.315 mg/mL fentanyl and 10 mg/mL fluanisone (Hypnorm; Janssen Pharmaceutical). On day 9, 1-mL blood samples were taken from the rabbits and a manual differential leukocyte count of these samples was performed. Then, both groups of rabbits received 20 MBq ^{99m}Tc-IL-8 (protein dose, 0.5 μg) via the ear vein. Three rabbits from each group were used for γ-camera imaging. These rabbits were immobilized in a mold and placed prone on the γ-camera; images were acquired at 0, 1, 2, and 4 h after injection with a single-head γ-camera (Orbiter; Siemens Medical Systems, Inc.) equipped with a parallel-hole, low-energy, all-purpose collimator. Images were obtained with a 15% symmetric window over the 140-keV energy peak of ^{99m}Tc. After acquisition of 100,000–300,000 counts, the images were digitally stored in a 256 × 256 matrix. Scintigraphic images were analyzed quantitatively by drawing regions of interest (ROIs) over the abscess and the contralateral thigh muscle (background). Abscess-to-background ratios were calculated.

After completion of the final imaging session (4 h after injection), all rabbits were killed with a lethal dose of sodium phenobarbital. Samples of blood, infected thigh muscle, uninfected contralateral thigh muscle, lung, spleen, liver, kidneys, and intestines were collected. The dissected tissues were weighed and the activity in the samples was measured in a γ-counter. To correct for radioactive decay, injection standards were counted simultaneously. The measured activity in samples was expressed as percentage of injected dose per gram of tissue (%ID/g). Abscess-to-contralateral muscle ratios and abscess-to-blood ratios were calculated.

For histologic examination, samples of infected thigh muscle of neutropenic and normal rabbits were fixed in formalin and embedded in paraffin. Sections (5 μm) were cut and stained with hematoxylin–eosin for light microscopic examination.

Mechanism of Migration of ^{99m}Tc-IL-8 from Circulation to Inflammatory Focus. The pharmacokinetics of ^{99m}Tc-IL-8 were determined in neutropenic and normal rabbits with turpentine-induced abscesses (3 rabbits per group). Multiple blood samples were collected between 1 min and 4 h after injection. Blood samples were weighed, their activity was measured, and their uptake was expressed as %ID/g and as %ID in the blood pool based on an estimated total blood volume of 6% of the total body weight of the rabbit (*17*).

The association of ^{99m}Tc-IL-8 with blood cells in circulation was studied after intravenous injection of radiolabeled IL-8. Blood

samples of 3 mL (in heparinized tubes) of 3 normal rabbits with turpentine-induced inflammation were taken at 5 min, 2 h, and 4 h after injection of the radiolabel. The blood was mixed with 0.75 mL of a dextran solution (6% dextran 500 [Pharmacia] in 0.9% NaCl) and allowed to sediment for 1 h at room temperature. The leukocyte-rich supernatant was carefully removed. The leukocyte-rich layer and the erythrocyte-rich layer were centrifuged for 15 min at 500*g*. The supernatants of both layers were removed and retained. The leukocyte pellet and the erythrocyte pellet were washed 3 times with 5 mL Hank's balanced salt solution and centrifuged for 10 min at 500*g*. The supernatants of all washing steps were retained. Radioactivity of the leukocyte pellet, the erythrocyte pellet, the plasma layer, and the supernatants of the washing steps was counted in a γ-counter. All radioactivity in the plasma layer and supernatants of the washing steps were taken together and designated as "plasma."

Kinetics of ^{99m}Tc-IL-8 In Vivo. Soft-tissue infections were induced in the left thigh muscle of 4 female New Zealand White rabbits (2.5–3.0 kg) with 1–2 × 10^{11} colony-forming units of *E. coli* in 0.5 mL. After 24 h, the rabbits were injected intravenously with ^{99m}Tc-IL-8. Scintigraphic images were obtained with a dual-head Siemens MultiSpect 2 γ-camera connected to a Scintiview image processor and ICON computer system (Siemens). All images were collected in digital format in a 256 × 256 matrix. Low-energy, parallel-hole collimators were used (140-keV photopeak, 15% symmetric window). Three rabbits were imaged alternately at a preset time of 10 min per image; 1 set of 3 images took approximately 35–40 min. In this way, 10 sets of whole-body images were generated between 0 and 6 h after injection. The animals were killed after completion of the last image, and tissue samples were collected, weighed, and counted in a γ-counter. Scintigraphic images were analyzed quantitatively by drawing ROIs over the abscess, contralateral thigh muscle, kidneys, bladder, liver, spleen, lungs and heart, and spine. In addition, regions were drawn near the organs for background correction.

The results of quantitative analysis of the images (in vivo biodistribution) were compared with the results of counting radioactivity in dissected tissues (ex vivo biodistribution) in an additional experiment. To ascertain whether in vivo biodistribution data are in accordance with ex vivo biodistribution data, 1 rabbit with an intramuscular infection was imaged on the dual-head Siemens MultiSpect 2 γ-camera as described above. After finishing the last image at 6 h after injection, the animal was killed and dissected. Radioactivity was counted in whole organs on a NaI crystal connected to a multichannel analyzer. Appropriate standards of injected dose (1%, 3%, 6%, 10%, 20%, and 30%) were counted as well. Special attention was paid to the analysis of radioactivity uptake in the infected hindleg. After counting radioactivity in the whole infected leg (similarly to drawing an ROI over the total high-uptake region), the leg was dissected stepwise in the direction of the central part of the abscess. The various dissected parts were weighed and counted. In this way, total %ID and %ID/g could be determined (ex vivo data). Similarly, abscess uptake was analyzed on the whole-body image, by drawing concentric regions around the central focus of the abscess (in vivo data). Ex vivo data were compared with in vivo data.

Statistical Analysis

All mean values are expressed as %ID/g, %ID, or ratios ± 1 SEM. Data were analyzed statistically using an unpaired *t* test (GraphPad Instat 3.00 Win 95; GraphPad Software, Inc.).

RESULTS

Specificity of Uptake of ^{99m}Tc-IL-8 in Abscess

Sections (5-μm; stained by hematoxylin–eosin) of the abscess of a normal, immunocompetent rabbit and a neutropenic rabbit are shown in Figure 1. Microscopic examination revealed a massive influx of predominantly polymorphonuclear cells (neutrophils) in the abscesses of normal rabbits (Fig. 1A). Remarkably, in neutropenic rabbits, the abscesses were also characterized by high numbers of infiltrating cells. However, in these animals the invading leukocytes were predominantly mononuclear—that is, lymphocytes and monocytes (Fig. 1B).

The reduction of neutrophil counts markedly affected the biodistribution of ^{99m}Tc-IL-8 in these rabbits as shown in Table 1 and Figure 2. Two cytarabine-treated rabbits were designated as "semineutropenic rabbits" because of higher neutrophil levels compared with those of 3 deeply neutropenic rabbits (8% and 19% vs. 4%, 0%, and 1%, respectively). These semineutropenic rabbits showed higher abscess uptakes than the deeply neutropenic rabbits. Abscess uptake correlated well with neutrophil counts in the cytarabine-treated and nontreated animals ($r = 0.90$; data not shown). Figure 2 illustrates the dramatic impact of neutrophil reduction on uptake of ^{99m}Tc-IL-8 in the abscess: low

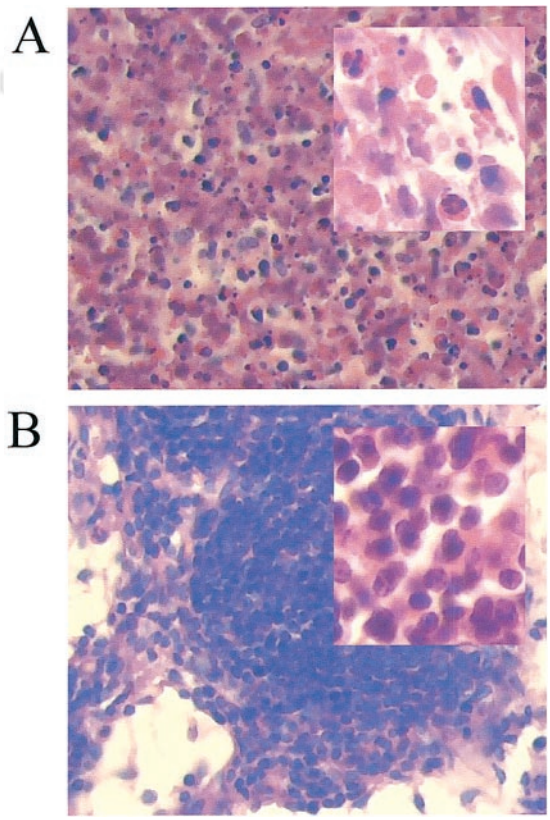

FIGURE 1. Stained tissues (hematoxylin–eosin) of turpentine-induced abscesses in normal, immunocompetent rabbit (A) and neutropenic rabbit (B). Note massive infiltration of polymorphonuclear cells (neutrophils) in A and mononuclear cells in B. (Hematoxylin–eosin, ×400 and ×1,000 [inset A, B])

TABLE 1
Biodistribution of ^{99m}Tc-IL-8 in Neutropenic and Normal Rabbits with Turpentine-Induced Abscesses

Biodistribution	Neutropenic rabbits (n = 3)	Normal rabbits (n = 4)
Blood	0.073 ± 0.004	0.069 ± 0.004
Muscle	0.005 ± 0.001	0.004 ± 0.001
Abscess	0.038 ± 0.014	0.41 ± 0.05
Lung	0.10 ± 0.02	0.34 ± 0.04
Spleen	0.38 ± 0.04	0.90 ± 0.08
Kidney	2.32 ± 0.30	2.13 ± 0.22
Liver	0.110 ± 0.024	0.080 ± 0.006
Intestine	0.044 ± 0.008	0.025 ± 0.002
Ratio		
Abscess/blood	0.5 ± 0.2	5.9 ± 0.7
Abscess/muscle	10 ± 5	110 ± 10
Target/background	1.2 ± 0.1	15 ± 1

Uptake is given as %ID/g. Values are expressed as mean ± 1 SEM.

abscess uptake in a neutropenic rabbit, moderate uptake in a semineutropenic rabbit, and high uptake in a normal rabbit. Association of ^{99m}Tc-IL-8 with neutrophils is demonstrated in Table 1: Abscess uptake is significantly higher ($P < 0.01$) in normal rabbits compared with that of neutropenic rabbits. Lung uptake is significantly higher ($P < 0.01$) in normal rabbits (0.34 %ID/g ± 0.04 %ID/g vs. 0.10 %ID/g ± 0.02 %ID/g). Uptake in the spleen is also significantly higher ($P < 0.01$) in normal rabbits (0.90 %ID/g ± 0.08 %ID/g vs. 0.38 %ID/g ± 0.04 %ID/g). These organs are known to accommodate high concentrations of neutrophils. Remarkably, uptake in intestinal tissue was significantly higher ($P < 0.05$) in neutropenic rabbits (0.044 %ID/g ± 0.008 %ID/g vs. 0.025 %ID/g ± 0.002 %ID/g). The abscess-to-blood, abscess-to-muscle, and target-to-background ratios from analysis of the images were significantly higher ($P < 0.01$, $P < 0.001$, $P = 0.0001$, respectively) for normal rabbits compared with those of the neutropenic ones.

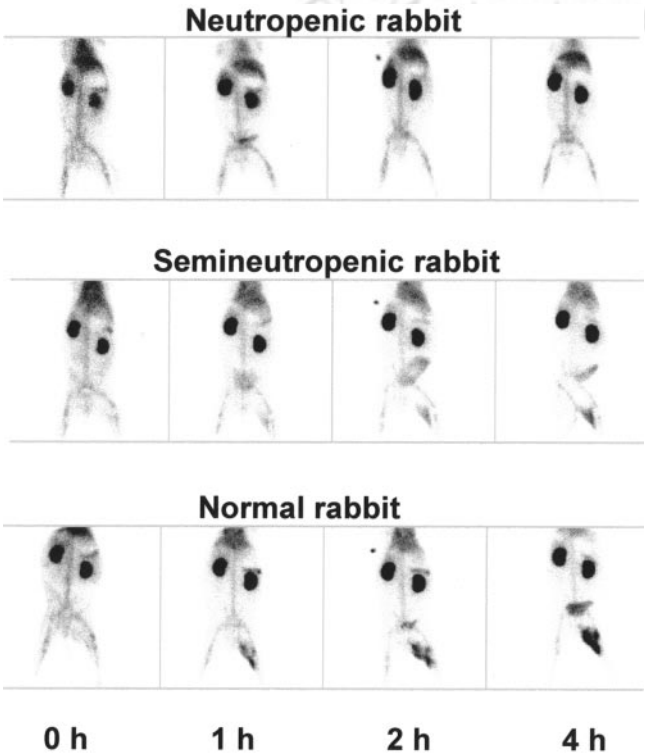

FIGURE 2. Images of rabbits with turpentine-induced abscesses in left thigh muscle at 5 min (0 h) and 1, 2, and 4 h after injection of ^{99m}Tc-IL-8. Neutrophil counts varied from very low levels (Neutropenic rabbit) via low levels (Semineutropenic rabbit) to normal levels (Normal rabbit).

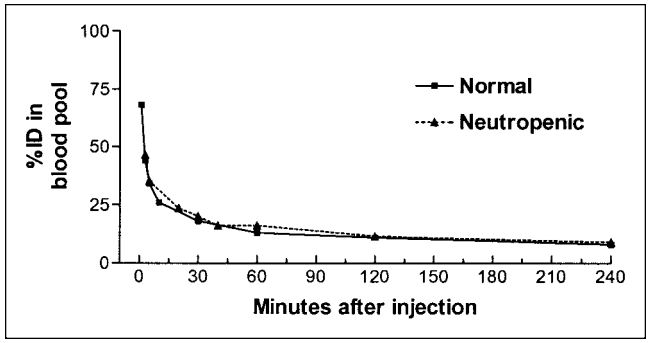

FIGURE 3. Blood clearance of ^{99m}Tc-IL-8 in normal, immunocompetent rabbits and in neutropenic rabbits with turpentine-induced inflammation. Data are expressed as %ID in blood pool.

Mechanism of Migration of ^{99m}Tc-IL-8 from Circulation to Inflammatory Focus

The blood clearance patterns of ^{99m}Tc-IL-8 in normal versus neutropenic rabbits with turpentine-induced soft-tissue abscesses were essentially congruent (Fig. 3), demonstrating that there is no major effect of the reduction of the number of neutrophils in circulation on the blood clearance of ^{99m}Tc-IL-8. The association of ^{99m}Tc-IL-8 with blood cells in samples of normal rabbits with turpentine-induced abscesses is shown in Table 2. The major fraction of the

TABLE 2
Distribution of ^{99m}Tc-IL-8 over Red Blood Cells, White Blood Cells, and Plasma in Normal Rabbits with Turpentine-Induced Abscesses

Time after injection	Plasma (%)	RBCs (%)	WBCs (%)
5 min	68 ± 2	31 ± 2	0.3 ± 0.02
2 h	68 ± 4	30 ± 4	2.3 ± 0.2
4 h	76 ± 4	23 ± 4	0.8 ± 0.2

RBC = red blood cell; WBC = white blood cell.
From blood samples at 3 different time points. Values are expressed as mean ± 1 SEM.

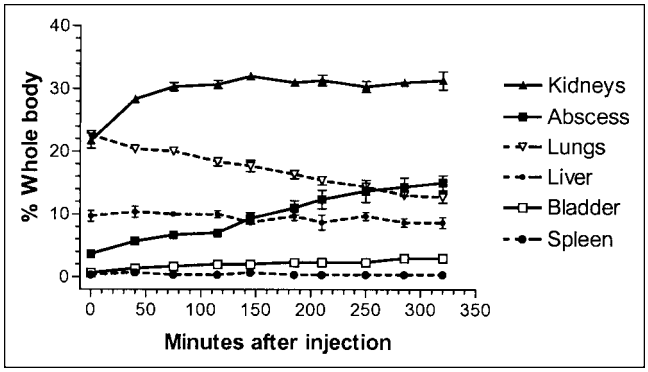

FIGURE 4. Kinetics of in vivo distribution of ^{99m}Tc-IL-8 in rabbits with *E. coli*-induced infection as determined by quantitative analysis of images. Uptake is quantified as percentage of whole-body activity. Error bars indicate ±SEM.

radiolabel was found in the plasma fraction, ranging from 68% immediately after injection to 76% at the last time point. Less than one third of the radiolabel was associated with red blood cells, and only a very low percentage (<2.5%) was associated with white blood cells.

Kinetics of ^{99m}Tc-IL-8 In Vivo

The kinetics of the in vivo distribution of ^{99m}Tc-IL-8 in rabbits with *E. coli*-induced infection are summarized in Figure 4. The whole-body activity ([WBA] corrected for physical decay) did not decrease. Therefore, during the experiment, radioactivity was not excreted from the body. An example of a posterior image with ROIs drawn is given in Figure 5. Analysis of the images showed a gradual increase in abscess uptake up to 15% ± 1% WBA at 5.5 h after injection. At that time, maximum uptake was not reached yet. Kidney uptake reached high levels immediately after injection of the radiolabel and remained stable from 1 h onward at a level of approximately 30% WBA. Uptake in the lungs showed a gradual decrease from a high level of uptake immediately after injection (23% ± 0.5% WBA) toward a moderate level at 5.5 h after injection (13% ± 1% WBA). Liver uptake was nearly stable over time at approximately 10% WBA. Spleen uptake appeared to be marginal in this experiment, <1% WBA at all time points. Activity in the bladder was low and did not exceed 3% ± 1% WBA at 5.5 h after injection. In addition, ROIs of spine and corresponding background areas were drawn, revealing only marginal uptake in the spine area (data not shown). A substantial amount of uptake was observed in the region of the head and forelegs, declining from 15% ± 1% WBA at the start to 9% ± 1% WBA at the end (not shown in Fig. 4). The major shifts in radioactivity distribution over time involved a clearance from the lungs (−10% WBA), the head and forelegs (−6% WBA), and the trunk (minus organs) in favor of kidney (+9% WBA) and the abscess (+12% WBA).

The results of a detailed analysis (both ex vivo and in vivo) of uptake of ^{99m}Tc-IL-8 in 1 rabbit are presented in Table 3 and Figure 5. ROIs were drawn as shown in Figure 6. Data of ex vivo and in vivo analysis showed a fair congruency. Ex vivo analysis displayed a gradual increase in radioactivity concentration (%ID/g) toward the core of the abscess. Taking into account considerably large uptakes in concentric areas around this abscess core, a total uptake of 17.6 %ID in the affected leg was determined. Similarly, in vivo analysis displayed a gradual increase in target-to-background ratios toward the center of inflammation, from 8.1 (abscess total), 14.2 (abscess periphery), up to 20.0 (abscess core). Total uptake in the affected leg (designated as abscess total) amounted to 18.5% WBA, based on ROI analysis, compared with 17.6 %ID from the ex vivo analysis.

DISCUSSION

The specific uptake of ^{99m}Tc-IL-8 in inflamed tissue is assumed to be based on high-affinity binding to IL-8 receptors on neutrophils. Neutrophil-driven specificity can be demonstrated in various ways—first, by studying the behavior of a control protein with similar size and charge but with no specific interaction with receptors on neutrophils. The observation in a previous study that abscess uptake of ^{99m}Tc-IL-8 was >10 times higher than abscess uptake of ^{99m}Tc-lysozyme suggested that abscess uptake was a result of the interaction of IL-8 with its receptors in inflammatory foci (*11*). An alternative way to demonstrate specific uptake is in vivo receptor blocking using an excess of unlabeled IL-8 or an excess of receptor-blocking monoclonal antibodies. However, saturation of receptors before injection of ^{99m}Tc-IL-8 is not feasible because excessive amounts of

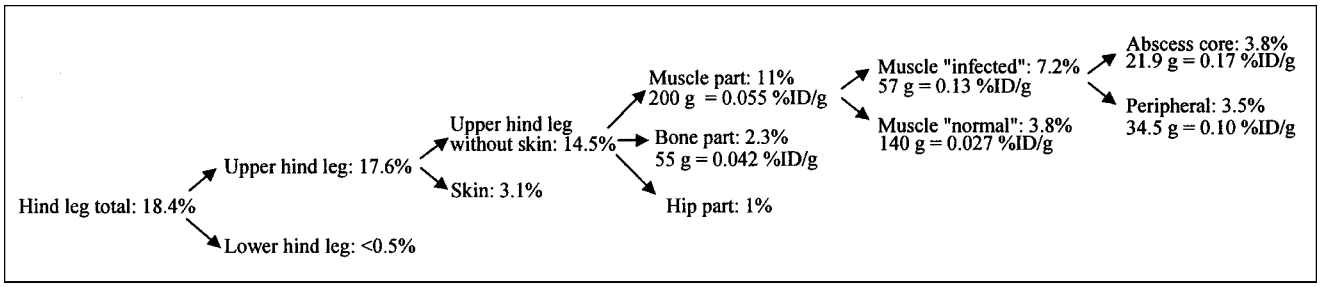

FIGURE 5. Detailed ex vivo analysis of uptake of ^{99m}Tc-IL-8 in *E. coli*-infected hindleg of New Zealand White rabbit at 6 h after injection. Uptake is given as %ID and as %ID/g for central parts of the affected muscle (compare with in vivo data, Table 3).

TABLE 3
Detailed Analysis of Uptake of ^{99m}Tc-IL-8 in *E. coli*-Infected Hindleg of New Zealand White Rabbit

Dissected parts	Ex vivo data (%ID)	ROI	In vivo data (% whole body)
Abscess core	3.8	Abscess core	4.5
Muscle part	11	Abscess peripheral	12.2
Upper hindleg	17.6	Abscess total	18.5
Kidney, left	14.4	Kidney, left	13.2
Kidney, right	15.4	Kidney, right	15.1
Liver	8.6	Liver	9.7
Spleen	0.75	Spleen	0.60
Lungs	4.4	Lungs	3.9

Comparison of radioactivity uptake in whole unfragmented organs and abscess parts (ex vivo analysis; Fig. 5) with uptake as determined by quantitative analysis of images at 6 h after injection. Ex vivo data are expressed as %ID; in vivo data are expressed as percentage of WBA.

unlabeled IL-8 will generate unacceptable biologic effects or would require excessive amounts of costly monoclonal antibodies. In this study, an alternative approach was chosen: comparing abscess uptake of ^{99m}Tc-IL-8 in neutropenic rabbits with that in rabbits with normal numbers of neutrophils. Microscopic examination of inflamed muscular tissue samples showed a shift in infiltrating leukocyte populations from predominantly polymorphonuclear cells (i.e., neutrophils) in normal rabbits to mononuclear cells (lymphocytes, monocytes) in cytarabine-pretreated rabbits. Patel et al. demonstrated that activated neutrophils express high numbers of CXCR1 and CXCR2 receptors (10^4 per cell), whereas activated mononuclear cells express low numbers of these receptors ($<10^2$ per cell) (*1*). As a consequence, the number of available receptors for ^{99m}Tc-IL-8 is greatly reduced in neutrophil-depleted rabbits. Accordingly, the uptake of ^{99m}Tc-IL-8 in the abscess was dramatically reduced in neutrophil-depleted rabbits. More precisely, a good correlation between neutrophil counts and abscess uptake was found ($r = 0.90$). The specific involvement of ^{99m}Tc-IL-8 with neutrophils was also reflected in high uptake in neutrophil-abundant organs such as lungs and spleen. Low uptake in neutrophil-depleted animals in these organs and in the abscess strongly suggests that accumulation of ^{99m}Tc-IL-8 is a neutrophil-driven process. Only a minor fraction of ^{99m}Tc-IL-8 localizes in the abscess nonspecifically. In neutropenic rabbits, uptake of ^{99m}Tc-IL-8 in the abscess is only 10% compared with abscess uptake in normal rabbits (Table 1) but is still 10 times as high as uptake in the contralateral muscle. A similar uptake pattern was seen for ^{99m}Tc-lysozyme in a previous study (*11*), suggesting again that some 10% of uptake of the radiolabel in the abscess could be ascribed to nonspecific uptake.

The mechanism of migration of ^{99m}Tc-IL-8 from the circulation to the focus of inflammation was the second focus of investigation. Several mechanisms of transportation can be conceived, grossly divided into neutrophil-bound transportation and nonneutrophil-bound transportation. Neutrophil-bound transportation involves high-affinity binding of ^{99m}Tc-IL-8 to receptors on peripheral neutrophils, followed by migration of the labeled cells to the inflamed tissue and passage through the endothelium. Nonneutrophil-bound transportation involves freely circulating ^{99m}Tc-IL-8 that extravasates and is subsequently trapped by receptors on infiltrated neutrophils. In addition, it has been shown that ^{99m}Tc-IL-8 can bind to some degree to receptors on red blood cells with low affinity (*18*). Our study pointed out that some 30% of the injected ^{99m}Tc-IL-8 was bound to red blood cells. The binding to red blood cells is rapidly reversible, and dissociation of ^{99m}Tc-IL-8 from the binding site on red blood cells is supposed to take place at the site of inflammation, where ^{99m}Tc-IL-8 is exposed to massive numbers of high-affinity binding sites on neutrophils (*8,18*).

Only a very low percentage of ^{99m}Tc-IL-8 in blood samples was associated with white blood cells. This observation is in favor of a nonneutrophil-bound transportation mechanism. On the other hand, several observations support the concept of neutrophil-bound transportation. Blood clearance of ^{99m}Tc-IL-8 in rabbits with turpentine-induced soft-tissue abscess showed a fast initial clearance (Fig. 3) within the first hour after injection, whereas the time period of highest increase in uptake

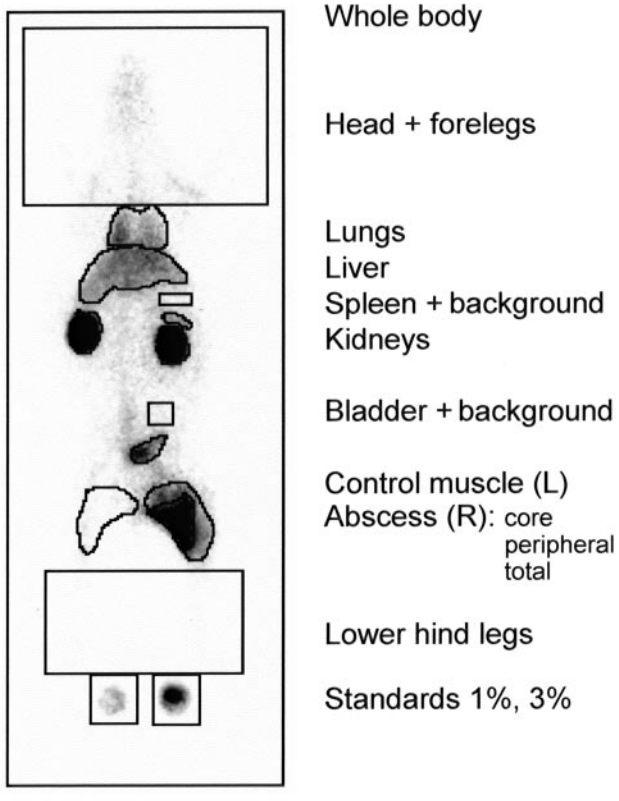

FIGURE 6. Typical example of ROIs in image of rabbit with *E. coli*-induced intramuscular infection injected with ^{99m}Tc-IL-8.

of ^{99m}Tc-IL-8 in the abscess was between 2 and 5 h after injection (Fig. 4). Uptake during that time period increased from 7% to approximately 15% of the injected dose. This observation, that the major part of ^{99m}Tc-IL-8 accumulates in the abscess in the time period that ^{99m}Tc-IL-8 has cleared (almost) completely from the blood, argues against nonneutrophil-bound transportation of ^{99m}Tc-IL-8 to the abscess. Furthermore, quantitative analysis of the images at various time points revealed that the accumulation of ^{99m}Tc-IL-8 in the abscess is accompanied by a simultaneous clearance of activity from the lungs, suggesting that neutrophil-associated ^{99m}Tc-IL-8 that is trapped in the lungs initially migrates to the abscess at later time points, favoring neutrophil-bound transportation from the lungs to the abscess. It has been shown that IL-8 can induce stiffening of neutrophils by reorganization of intracellular actin, and this could explain the leukosequestration in the lungs. These cells lose their flexibility and, consequently, cannot pass the narrow microcapillaries of the lungs anymore (*19*,*20*). Because leukosequestration is a transient phenomenon, neutrophils (with adherent radiolabel) gradually reenter circulation and subsequently migrate to the inflamed tissue because of their enhanced chemotactic status induced by IL-8. Between injection and the final imaging, the lung uptake decreased by 10%, while the abscess uptake increased by 12%. It is tempting to speculate that increasing abscess uptake could, in part, be ascribed to a continuous supply of radiolabeled neutrophils from the lungs.

Furthermore, several studies have shown that infiltrated (phagocytosing) neutrophils (*21*) in inflamed tissue in an environment of high concentrations of chemotactic cytokines (*22*) (and microorganisms (*23*) or products thereof (*24*)) have downregulated their CXCR1 and CXCR2 expression and express relatively low numbers of these receptors, further arguing against direct targeting of infiltrated neutrophils by ^{99m}Tc-IL-8. It is plausible that ^{99m}Tc-IL-8 targets predominantly peripheral neutrophils and not neutrophils within the inflammatory lesion.

On the basis of these considerations, we propose the following hypothesis. Upon intravenous injection, ^{99m}Tc-IL-8 is partly bound to peripheral neutrophils and the major fraction of ^{99m}Tc-IL-8 remains unbound. The fast blood clearance of the radiolabel mainly reflects the fast pharmacokinetics of the unbound ^{99m}Tc-IL-8 fraction. Unbound ^{99m}Tc-IL-8 is rapidly cleared predominantly by the kidneys. Not surprisingly, the blood clearance patterns in normal versus neutropenic rabbits are essentially congruent, as these are both reflecting unbound ^{99m}Tc-IL-8. The neutrophils that bind ^{99m}Tc-IL-8 stiffen and are trapped in the microcapillaries of the lungs. After release from the lungs, these cells migrate to the inflamed tissue and extravasate at the site of infection in a highly selective way. Because the release of the cells from the lungs is a gradual process, the analysis of blood samples reveals only a low percentage of the radiolabel attached to white blood cells. Analysis of blood samples mainly reflects unbound ^{99m}Tc-IL-8. Quantitative analysis of images reveals the comparatively slow pharmacokinetics of the cell-bound ^{99m}Tc-IL-8 fraction.

Accumulation of ^{99m}Tc-IL-8 in the abscess is a neutrophil-driven gradual process, highly specific and efficient. ^{99m}Tc-IL-8 accumulated in abscesses of immunocompetent rabbits to a very high degree as determined by quantitative analysis of images and ex vivo quantification. In vivo biodistribution data did not conflict with ex vivo biodistribution data, showing the reliability of both approaches. The results showed that in previous studies (*11*,*14*) the total ex vivo abscess uptake of ^{99m}Tc-IL-8 was underestimated. Apparently, in the earlier studies, only a part of the inflamed tissue was dissected and analyzed.

CONCLUSION

In this study, substantial support is provided in favor of the hypothesis that ^{99m}Tc-IL-8 localizes in the abscess mainly due to neutrophil-bound transportation. Accumulation of ^{99m}Tc-IL-8 in the abscess is a neutrophil-driven process, highly specific and efficient: Abscess uptake in immunocompetent rabbits with intramuscular infection is extremely high (up to >15%ID), as confirmed by in vivo and ex vivo analysis. On the basis of experimental data, ^{99m}Tc-IL-8 meets virtually all desiderata for successful imaging of infection and inflammation: High and highly specific uptake in abscesses, fast clearance from nontarget tissues, and low protein doses are promising features for the introduction of ^{99m}Tc-IL-8 into the clinic.

ACKNOWLEDGMENTS

The authors thank Gerry Grutters and Hennie Eikholt (Central Animal Laboratory, University Medical Center Nijmegen) for their excellent technical assistance in the animal experiments, Trix de Boer (Department of Hematology, University Medical Center Nijmegen) for the microscopic examination and evaluation of blood and tissue samples, and Theo Smedes for his valuable assistance in carrying out the experiments.

REFERENCES

1. Patel L, Charlton SJ, Chambers JK, Macphee CH. Expression and functional analysis of chemokine receptors in human peripheral blood leukocyte populations. *Cytokine.* 2001;14:27–36.
2. Holmes WE, Lee J, Kuang WJ, Rice GC, Wood WI. Structure and functional expression of a human interleukin-8 receptor. *Science.* 1991;253:1278–1280.
3. Murphy PM, Tiffany HL. Cloning of complementary DNA encoding a functional human interleukin-8 receptor. *Science.* 1991;253:1280–1283.
4. Lee J, Horuk R, Rice GC, Bennett GL, Camerato T, Wood WI. Characterization of two high affinity human interleukin-8 receptors. *J Biol Chem.* 1992;267: 16283–16287.
5. Cerretti DP, Kozlosky CJ, Vanden Bos T, Nelson N, Gearing DP, Beckmann MP. Molecular characterization of receptors for human interleukin-8, GRO/melanoma growth-stimulatory activity and neutrophil activating peptide-2. *Mol Immunol.* 1993;30:359–367.
6. Hay RV, Skinner RS, Newman OC, et al. Scintigraphy of acute inflammatory lesions in rats with radiolabelled recombinant human interleukin-8. *Nucl Med Commun.* 1997;18:367–378.
7. van der Laken CJ, Boerman OC, Oyen WJ, van de Ven MT, van der Meer JW, Corstens FH. Radiolabeled interleukin-8: specific scintigraphic detection of infection within a few hours. *J Nucl Med.* 2000;41:463–469.

8. van der Laken CJ, Boerman OC, Oyen WJ, van de Ven MT, Ven der Meer JW, Corstens FH. The kinetics of radiolabelled interleukin-8 in infection and sterile inflammation. *Nucl Med Commun.* 1998;19:271–281.
9. Gross MD, Shapiro B, Fig LM, Steventon R, Skinner RW, Hay RV. Imaging of human infection with ^{131}I-labeled recombinant human interleukin-8. *J Nucl Med.* 2001;42:1656–1659.
10. Rennen H, Boerman O, Oyen W, Corstens F. Labeling method largely affects the imaging potential of interleukin-8 [letter]. *J Nucl Med.* 2002;43:1128.
11. Rennen HJ, Boerman OC, Oyen WJ, van der Meer JW, Corstens FH. Specific and rapid scintigraphic detection of infection with ^{99m}Tc-labeled interleukin-8. *J Nucl Med.* 2001;42:117–123.
12. Gratz S, Rennen HJ, Boerman OC, Oyen WJ, Burma P, Corstens FH. ^{99m}Tc-Interleukin-8 for imaging acute osteomyelitis. *J Nucl Med.* 2001;42:1257–1264.
13. Gratz S, Rennen HJ, Boerman OC, Oyen WJ, Corstens FH. Rapid imaging of experimental colitis with ^{99m}Tc-interleukin-8 in rabbits. *J Nucl Med.* 2001;42: 917–923.
14. Rennen HJ, van Eerd JE, Oyen WJ, Corstens FH, Edwards DS, Boerman OC. Effects of coligand variation on the in vivo characteristics of Tc-99m-labeled interleukin-8 in detection of infection. *Bioconjug Chem.* 2002;13:370–377.
15. Abrams MJ, Juweid M, tenKate CI, et al. Technetium-99m-human polyclonal IgG radiolabeled via the hydrazino nicotinamide derivative for imaging focal sites of infection in rats. *J Nucl Med.* 1990;31:2022–2028.
16. Schwartz DA, Abrams MJ, Giadomenico CM, Zubieta JA, inventors; Johnson Matthey, Inc., assignee. Certain pyridyl hydrazines and hydrazides useful for protein labeling. US patent 5 206 370. April 27, 1993.
17. Jain NC. Blood volume and water balance. In: Jain NC, ed. *Schalm's Veterinary Hematology.* Philadelphia, PA: Lea & Febiger; 1986:87–102.
18. Darbonne WC, Rice GC, Mohler MA, et al. Red blood cells are a sink for interleukin 8, a leukocyte chemotaxin. *J Clin Invest.* 1991;88:1362–1369.
19. Worthen GS, Schwab B III, Elson EL, Downey GP. Mechanics of stimulated neutrophils: cell stiffening induces retention in capillaries. *Science.* 1989;245:183–186.
20. Drost EM, MacNee W. Potential role of IL-8, platelet-activating factor and TNF-alpha in the sequestration of neutrophils in the lung: effects on neutrophil deformability, adhesion receptor expression, and chemotaxis. *Eur J Immunol.* 2002;32:393–403.
21. Doroshenko T, Chaly Y, Savitskiy V, et al. Phagocytosing neutrophils down-regulate the expression of chemokine receptors CXCR1 and CXCR2. *Blood.* 2002;100:2668–2671.
22. Feniger-Barish R, Belkin D, Zaslaver A, et al. GCP-2-induced internalization of IL-8 receptors: hierarchical relationships between GCP-2 and other ELR(+)-CXC chemokines and mechanisms regulating CXCR2 internalization and recycling. *Blood.* 2000;95:1551–1559.
23. Tikhonov I, Doroshenko T, Chaly Y, Smolnikova V, Pauza CD, Voitenok N. Down-regulation of CXCR1 and CXCR2 expression on human neutrophils upon activation of whole blood by S. aureus is mediated by TNF-alpha. *Clin Exp Immunol.* 2001;125:414–422.
24. Khandaker MH, Xu L, Rahimpour R, et al. CXCR1 and CXCR2 are rapidly down-modulated by bacterial endotoxin through a unique agonist-independent, tyrosine kinase-dependent mechanism. *J Immunol.* 1998;161:1930–1938.